

Chemical imaging of pharmaceuticals by time-of-flight secondary ion mass spectrometry

S.Y. Luk,^a N. Patel^a and M.C. Davies^b

^a*Molecular Profiles Ltd, 1 Faraday Building, Nottingham Science & Technology Park, University Boulevard, Nottingham NG7 2QP, UK. E-mail: sluk@molprofiles.co.uk*

^b*Laboratory of Biophysics and Surface Analysis, School of Pharmaceutical Sciences, University of Nottingham, Nottingham NG7 2RD, UK*

Introduction

Oral solid dosage formulations (for example, tablets and pellets) are a convenient method of drug delivery and account for a large proportion of pharmaceutical products. Drug substances are not routinely administered in the pure state, and functional components (bulking agents, processing aids etc.) are commonly used. Thus, even the simplest of tablets will be a heterogeneous mixture of many components, with individual particles often of the order of micrometres in size. Additionally, solid dosage design can include strategies to control the rate of drug delivery (for example, sustained release), typically using one or more polymer coatings. This has added an extra level of complexity in formulation design. To aid the formulator, supporting information by way of detailed analysis of the final product is vital. The direct analysis of these complex systems has been addressed in the past twenty years or so by the advent of chemical spectroscopy/spectrometry techniques allowing chemical mapping. Of these, the Raman microprobe and infrared microscopy are clearly capable of giving significant levels of spatially-resolved chemical information.¹ However, chemical mapping using time-of-flight secondary ion mass spectrometry (ToF-SIMS) not only provides complementary information to these vibrational spectroscopy techniques, but also has clear additional advantages in terms of spatial resolution (<1 μm) and sensitivity (<ppm) as well as providing information on the chemistry of the surface at specific locations of interest.² In this article, a brief overview of ToF-SIMS methodology is presented. The applications of this technique to study the dis-

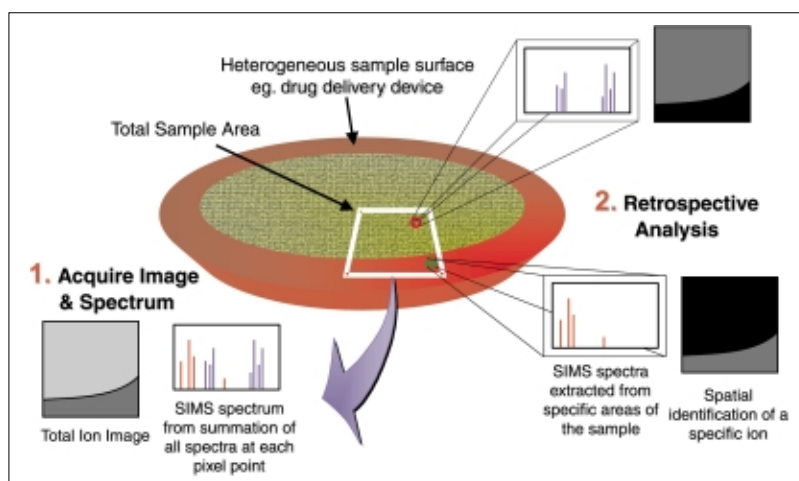


Figure 1. Schematic of ToF-SIMS analysis mode of a coated bead. (1) Generation of a total ion image and total area spectrum obtained during data acquisition. (2) Extraction of either a spectrum from a region of interest or an ion map leading to chemical images.

tribution of components within complex heterogeneous systems such as controlled release beads will be highlighted with two examples. A more detailed account of the techniques and application of ToF-SIMS to pharmaceutical products described here can be found in Reference 3.

Basis of chemical imaging using MS

The SIMS process involves bombarding the sample surface with a beam of primary ions (e.g. gallium or caesium). Collision of the beam with the surface results in emission of secondary particles populated by electrons, atoms, neutral molecules and ions (positively

and negatively charged). The latter can be mass analysed leading to useful chemical information. Intrinsicly the ion beam is a destructive method of generating ions but by carefully rastering an ion beam of sufficiently low current, it is possible to derive data from effectively a pristine surface. This mode, termed *static* SIMS, offers a route to detailed mass analysis of the surface monolayer in an unperturbed state.⁴ By acquiring a mass spectrum from points as the beam traverses the sample surface, a two-dimensional array of mass spectra is produced, Figure 1. This data set can now be treated in a variety of ways. By analysing the summed mass spectra, specific ions can be assigned to components of interest, and the distribution of these can then be determined by mapping the intensity spatially. Alternatively, from the ion image, mass

spectra from regions of interest can be extracted to determine composition from selected areas.

Experimental

Two drug loaded beads were prepared by extrusion/spheronisation and then subsequently coated by modified release polymers using fluid bed coating apparatus. Example 1 comprised of prednisolone sodium metasulfobenzoate dispersed in Avicel™ (a microcrystalline cellulose) and lactose. This was then coated with Surelease (a controlled release polymer based on ethylcellulose) and amylose. Example 2 comprised of theophylline dispersed in Avicel™ and lactose, and coated with Eudragit L30-D (an enteric coating based on a methacrylic acid/ethyl acrylate copolymer and talc; an enteric coating is an acid insoluble polymer based coating designed to prevent tablet or pellet disintegration in the acid environment of the stomach). Prior to analysis the beads were bisected to expose the interior. ToF-SIMS was performed using a Physical Electronics TRIFT II. Under imaging mode, the instrument employed a Ga⁺ source operating at 25 keV with 20 ns pulses.

Results

In Figure 2(a), a total ion image of a whole bead (approximately 800 μm diameter) from Example 1 is shown. Here, the image is presented using a “thermal” colour scale, and the increased intensity (yellow) reflects the higher ion yield from the components found in the core compared to the surrounding coating polymer (red). The image shows clearly the integrity and uniformity of the polymer coating over the entire circumference of the bead.

From the box highlighted, a higher resolution total ion image of the outer region is shown in Figure 2(b), and the discrete particulate morphology of the core compared to the smoother texture of the polymer coating allows differentiation between these two areas. An example of the utility of data processing post acquisition can now be shown with this data set. Having established the level of heterogeneity between the core and coating from the total ion image, it is now possible to determine chemical composition through spectroscopy in these two regions. Within Figure 2(b), regions of interest can be defined and a summation of all the spectra contained in the boundary gives mass spectra solely from either the polymer coat region, Figure 2(c), or the core region, Figure 2(d), which can then be compared against reference spectra. In the core,

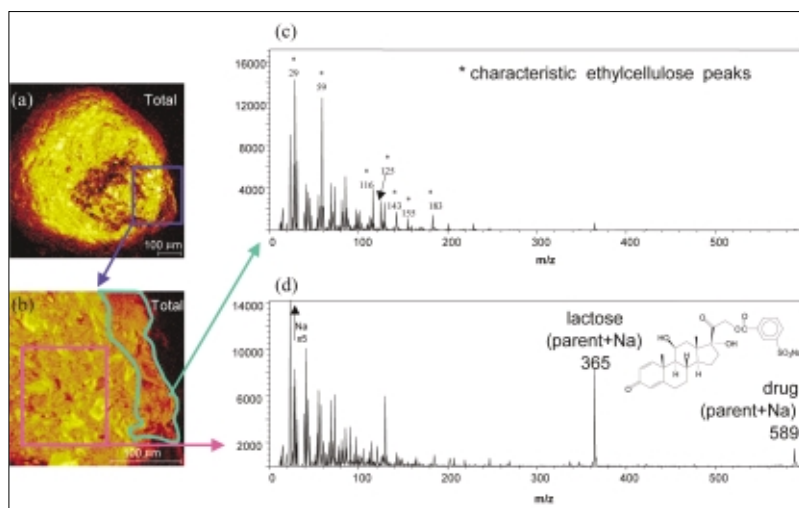


Figure 2. (a) ToF-SIMS total ion image of Example 1 bead cross-section and close-up (b) of highlighted region. Mass spectra from (c) coating region (green) and (d) core region (pink) showing distinct differences between these two regions. Reprinted with permission from M.C. Davies *et al.*, *Anal. Chem.* 72(22), 5631, Copyright (2000) American Chemical Society.

the peak at m/z 589 can be assigned to the prednisolone metasulfobenzoate ($[C_{21}H_{31}O_9S]^+$) cation and the peak at m/z 365 assigned to Na⁺ cationised lactose ($[C_{12}H_{22}O_{11}] + Na^+$). Compared to the other components within the core, Avicel™ (a microcrystalline cellulose) gives a relatively low ion yield of low mass fragment species and so is not easily detected amongst the lactose and drug signals. In the spectrum derived from the polymer coating, the main peaks are associated with the low mass fragments from the ethylcellulose component, in particular the ethyl ether group (m/z 59, $CH_3CH_2OCH_2^+$).

Having established “marker” ions, a distribution of drug, lactose and polymer coating can be determined by composing an image of ion intensity for these particular components, Figure 3. The distribution of the individual components are indicated by Figure 3(a) (ethyl cellulose, m/z 59), Figure 3(b) (lactose, m/z 365) and Figure 3(c) (prednisolone, m/z 589) and their relative distribution in the overlay image of these three components, Figure 3(d). From these images, the size and distribution of the lactose particles (5–30 μm) and prednisolone metasulfobenzoate (present in domains up to 20 μm) are determined and located solely in the core as anticipated. Ethylcellulose forms a discrete and intact coating, approximately 50 μm thick. Furthermore, a well-defined interface between the core/coating with no intermixing between the core and coating are evident.

In Example 2, an enteric coated theophylline bead, the total ion image of a bead quadrant, Figure 4(a), shows

the core/coating morphology with a higher intensity of ions originating from the core compared to the polymeric coating providing the contrast mechanism. In the core, the distribution of the theophylline can be readily determined from the image of the protonated molecular ion m/z 181, Figure 4(b), and compared to the previous example shows a much more homogeneous distribution. This is probably due to the solubility of theophylline in water used in the extrusion spheronisation method of preparing the core, which may distribute the theophylline through solvation and precipitation in the excipient blend. Additionally, an image of the m/z 365 [Figure 4(c)], Na⁺ cationised lactose as before, shows enrichment at the outermost part of the core. This segregation may again be a result of the water-based extrusion spheronisation process used in manufacture of the bead cores. In determining the integrity of the coating layer, whilst peaks associated with the polymer are present (assigned principally to the monomer in the positive ion spectrum), peaks assigned to Mg at m/z 24, from the talc (magnesium silicate) are dominant. An image of the m/z 24 peak, Figure 4(d), clearly shows the presence of a discrete layer (approximately 15 μm thick) encapsulating the core. This exemplifies an important feature of SIMS, where inorganic as well as organic species can be analysed and imaged.

Although the cores of the two examples presented here are prepared by extrusion spheronisation, the distribution of the drug and excipients are markedly different, as demonstrated by ToF-SIMS chemical mapping. Addi-

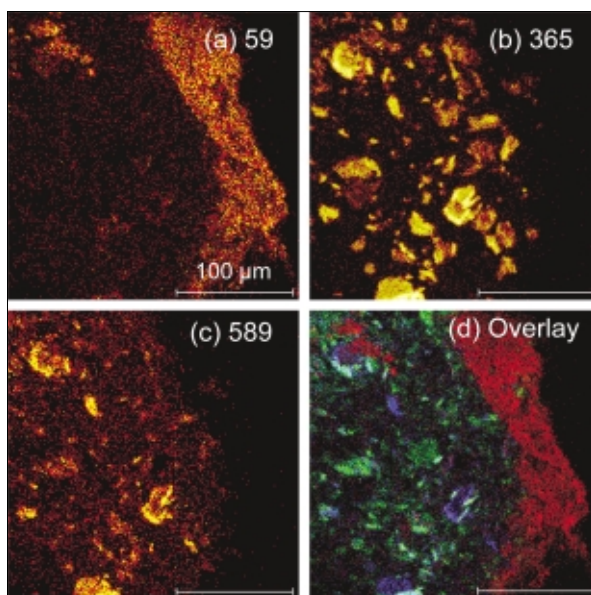


Figure 3. ToF-SIMS images of Example 1 ($250\ \mu\text{m} \times 250\ \mu\text{m}$), showing distribution of m/z 59, 365 and 589 and overlay, assigned to ethyl cellulose (red), lactose (green) and prednisolone drug (blue). Reprinted in part with permission from M.C. Davies *et al.*, *Anal. Chem.* 72(22), 5632, Copyright (2000) American Chemical Society.

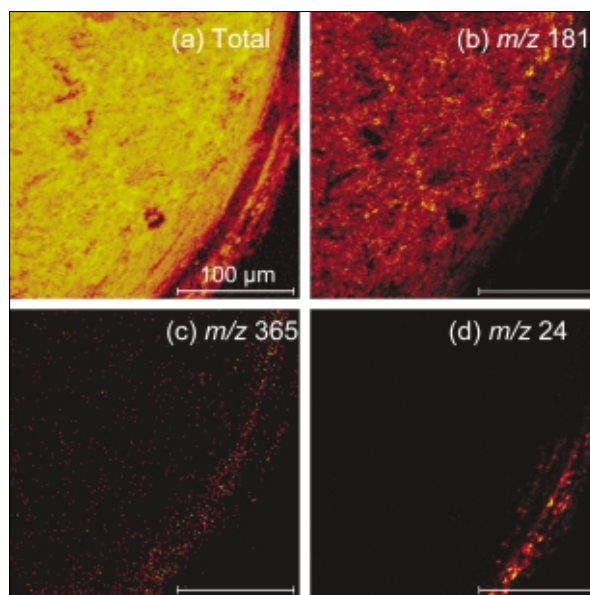


Figure 4. Ion images of Example 2 ($250\ \mu\text{m} \times 250\ \mu\text{m}$) showing (a) total ion image and distribution of (b) protonated drug molecular ion (m/z 181) (b) sodium cationised lactose (m/z 365) and (d) magnesium (m/z 24). Reprinted in part with permission from M.C. Davies *et al.*, *Anal. Chem.* 72(22), 5633, Copyright (2000) American Chemical Society.

ionally, the coatings were found to be coherent and of uniform thickness, even though the type of polymer was different. It is readily evident that chemical mapping by ToF-SIMS is a very powerful method of analysing complex pharmaceutical solid dosage systems.

Conclusions

The analysis of pharmaceutical solid dosage formulations is an excellent case study to illustrate the huge potential of chemical mapping by ToF-SIMS. The advantages of a chemical mapping technique with high spatial resolution ($<1\ \mu\text{m}$), high sensitivity ($<\text{ppm}$) and capability to detect both organic and inorganic species is made abundantly clear when faced with complex hetero-

geneous systems where individual components are of the micrometre scale. To this end, the pharmaceutical industry, along with many other branches of chemical manufacturing, is introducing evermore-complex functionality within products. ToF-SIMS has a considerable amount to offer in respect to the detailed analysis of these product innovations.

Acknowledgements

We thank Mike Newton (University College London) and Anna Belu (Medtronic) for their invaluable contributions.

References

1. Don Clark, "The Analysis of Pharmaceutical Substances and

Formulated Products by Vibrational Spectroscopy", in "Handbook of Vibrational Spectroscopy" Vol. 5, Ed by J.M. Chalmers and P.R. Griffiths. John Wiley & Sons, Chichester, pp 3574–3589 (2002).

2. M.C. Davies, K.M. Shakesheff, C.J. Roberts, S.J.B. Tendlar, S. Bryan and N. Patel in *The Encyclopedia of Controlled Drug Delivery*, Ed By E. Mathiowitz. John Wiley & Sons, New York, pp. 269–275 (1999).
3. A.M. Belu, M.C. Davies, J.M. Newton and N. Patel, *Anal. Chem.* 72(22), 5625 (2000).
4. D. Briggs and M.J. Hearn, *Vacuum* 36, 1005 (1986).